Overview of Model Test Procedures for Stability Under Dead Ship Condition and Pure Loss of Stability in Astern Waves

Naoya Umeda, Daichi Kawaida, Yuto Ito, Yohei Tsutsumi, Akihiko Matsuda, and Daisuke Terada

Abstract For facilitating the development of the guidelines for direct stability assessment as a part of the second generation intact stability criteria at the International Maritime Organization (IMO), this paper provides examples of comparison between model experiments and numerical simulations for stability under dead ship condition and pure loss of stability in astern waves. As a result, some essential elements for proper validation were identified. For dead ship stability, a good selection of representative wind velocity generated by wind fans is crucial. For pure loss of stability, accurate Fourier transformation and reverse transformation of incident irregular waves are essential. These remarks were partly utilised in the interim guidelines as finalised in 2020.

Keywords Second generation intact stability criteria · Direct stability assessment · IMO · Dead ship condition · Pure loss of stability

1 Introduction

At the IMO, the second generation intact stability criteria, which consist of three-level criteria, are now under development. Here their highest level means direct stability assessment using time-domain numerical simulation tools, which should be validated with physical model experiments. For this purpose, the IMO started to develop the guidelines for direct stability assessment procedures under the initiative of the United States and Japan as SDC 1/INF. 8, annex 27 [8]. For finalising the

N. Umeda (✉) · D. Kawaida · Y. Ito · Y. Tsutsumi
Osaka University, Suita, Japan
e-mail: umeda@naoe.eng.osaka-u.ac.jp

A. Matsuda
Japan Fisheries Research and Education Agency, Kamisu, Japan
e-mail: amatsuda@fra.affrc.go.jp

D. Terada
National Defence Academy, Yokosuka, Japan
e-mail: dterada@nda.ac.jp

K. J. Spyrou et al. (eds.), *Contemporary Ideas on Ship Stability*, Fluid Mechanics and Its Applications 134, https://doi.org/10.1007/978-3-031-16329-6_36

guidelines, particularly their quantitative acceptance criteria, it is indispensable to examine their feasibility by comparing model experiments with numerical simulations. Thus, it is important to collect comparisons between model experiments and numerical simulations for the relevant stability failure modes.

The second generation intact stability criteria deal with five failure modes, i.e., parametric rolling, pure loss of stability in astern waves, broaching, stability under dead ship condition and excessive acceleration. Among them, a relatively large number of validation reports for parametric rolling (e.g. [6]) and broaching (e.g. [5]) are available, but only the limited number of reports for stability under dead ship condition [14] and pure loss of stability [13]. Since few published experimental data are available, even the experimental procedures for stability under dead ship condition have not yet been established by the International Towing Tank Conference [12].

Therefore, the authors attempted to validate numerical simulation codes for stability under dead ship condition in irregular beam wind and waves and pure loss of stability in irregular astern waves and published its report at the International Ship Stability Workshop as [19]. Some part of this information was used for the development of the IMO interim guidelines for direct stability assessment, which was circulated in 2020 [9]. This means that this work was based on the draft guidelines available in 2013, which was slightly different from the current guidelines finalized in 2020. The authors presume that it could facilitate the revision of the ITTC recommended procedures for intact stability model test in future.

2 Draft Guidelines of Direct Stability Assessment Procedures in 2013

The draft guidelines for direct stability assessment procedures drafted by the United States and Japan by 2013 consist of requirements for numerical modelling, qualitative and quantitative validation of software and extrapolation procedures. For the quantitative validation, numerically simulated results are requested to be compared with the model experiments based on the ITTC recommended procedures [12]. Its acceptance criteria are shown in Table 1. In this table, it was accepted in 2013 that all quantitative numbers that appeared as the acceptance standards here should be considered tentative unless sufficient evidence of their feasibility is submitted to the IMO. It is noteworthy here that these requirements do not refer to irregular wind at all. This is because it is not easy to find literature describing ship model experiments with artificial irregular wind and waves except for Kubo et al. [14]. It can also be remarked that no acceptance criteria for pure loss of stability in astern waves exist. This is because only recently the mechanism of "pure loss of stability" was discussed by Umeda et al. [18] and Kubo et al. [13]. They experimentally and numerically confirmed that large roll triggered by a loss of restoring moment due to longitudinal waves could usually induce lateral motions because of the asymmetric underwater hull due to

heel. Centrifugal force due to such lateral motions could induce further roll motion. Thus, the phenomenon known as "pure loss of stability" should be theoretically investigated with restoring reduction and centrifugal force due to lateral motions. These raised points have already been adopted by the IMO [9] for the vulnerability criteria as a part of the second generation intact stability criteria. Therefore, it is an urgent issue to provide examples of comparison in artificial irregular waves between model experiments and numerical simulation.

3 Stability Failure in Irregular Beam Wind and Waves

3.1 Experimental Procedures

For examining the validation procedures for stability under dead ship condition experiments using a 1/70 scaled model of the 205.7 m-long CEHIPAR2792 vessel [16] were conducted at the Marine Dynamics basin, shown in Fig. 1, of the National Research Institute of Fisheries Engineering [15]. The ship model has a flat plate on the upper deck for realising the windage area and its area centre height of the superstructure but without additional buoyancy. It was not equipped with bilge keels, propellers, shaft brackets and rudders. An optical fibre gyroscope inside the model is used for detecting the roll, pitch and yaw angles. For sway and heave motions, the total station system, which is described in Chap. 4, was used.

The model was kept orthogonal to the wind and wave direction by a wired system, which softly restrains drift and yaw, as shown in Figs. 2 and 3. The wind blows in one direction, and the long-crested wave propagated in the same direction. Here the wired system was connected to the ship model at bow and stern, where the height was set to be equal to calm water surface based on measured hydrodynamic reaction force and moment in a captive model test of the subject ship. As shown in Fig. 3, the mean of the low-frequency sway motion due to mean wind velocity and the second-order wave force was cancelled out by the tension due to a counterweight. Thus, high-frequency sway motion was not prevented. Alternatively, an automatic tension adjustment system using a constant torque motor can be introduced to cancel it out.

Irregular water waves were generated by plunger-type wavemakers with the ITTC wave energy spectrum recommended in 1978 [11]. The wave elevation was measured by a servo-needle-type wave height meter equipped in the sub towing carriage. Figure 4 shows one example of the comparison of wave energy spectra. The straight blue line indicates the specified spectrum in this figure, and the green square symbols indicate the measured one. From this figure, it can be seen that the specified spectrum was satisfactorily realized.

The fluctuating wind was generated by a wind blower in the wave direction. The wind blower, as shown in Fig. 5, consists of 36 axial flow fans and is controlled by inverters with a v/f control law, by which the ratio of primary voltage for the induced motor and the inverter output frequency is controlled to be constant.

Table 1 Quantitative validation requirements [8]

	Required for	Objective	Acceptance criteria
Response curve for parametric roll	Parametric roll and excessive accelerations	To demonstrate reasonable agreement between numerical simulation and the models test on both bandwidth of parametric resonance and the amplitude of the roll response	[1/10] of natural roll frequency for the bandwidth and [10%] of amplitude if below angle maximum of GZ curve in calm water and [20%] if above the angle of maximum of the GZ curve in calm water
Response curve for synchronous roll	All modes	To demonstrate reasonable agreement between numerical simulation and the models test on the amplitude of the roll response	[10%] of amplitude if below angle maximum of GZ curve in calm water and [20%] if above the angle of maximum of the GZ curve in calm water
[Turning circle maneuver	Software for numerical simulation of surf-riding and broaching	Demonstrate correct modeling of maneuvering forces and turn dynamics in calm water	[20%] difference in terms of diameter of turning circle between the model test and numerical simulation and the correct sign of drift angle
Zig-zag maneuver	Software for numerical simulation of surf-riding and broaching	Demonstrate correct modeling of maneuvering forces and turn dynamics in calm water	[10%] difference in terms of the 1st and second overshoot angles between the model test and numerical simulation]
Variance test/synchronous roll	Software for numerical simulation of dead ship condition and excessive accelerations	Demonstrate correct (in terms of statistics) modeling of roll response in irregular waves	Probability that the difference between the ensemble estimates of variance of roll is caused by the random reasons is above the significant level of [5%]
Variance test/parametric roll	Software for numerical simulation of dead ship condition and excessive accelerations	Demonstrate correct (in terms of statistics) modeling of roll response in irregular waves	Probability that difference between the ensemble estimates of variance of roll is caused by the random reasons is above the significant level of [1%]

(continued)

Table 1 (continued)

	Required for	Objective	Acceptance criteria
Wave conditions for surf-riding and broaching	Software for numerical simulation of surf-riding and broaching	Demonstrate correct modeling of surf-riding broaching dynamics in regular waves	Wave steepness causing surf-riding and broaching at the wave length [0.75–1.5] of ship length is within [15%] of difference between model test and numerical simulation; speed settings are also within [15%] difference between model test and numerical simulation

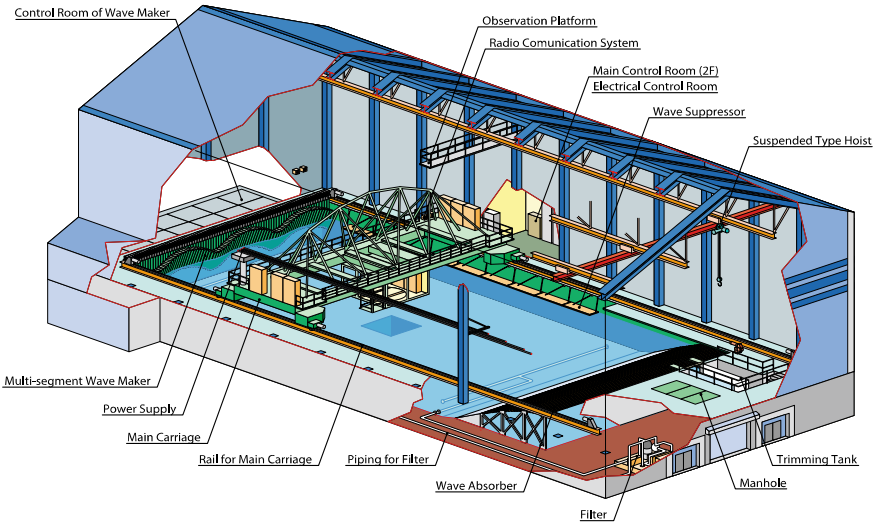

Fig. 1 Marine Dynamics Basin of National Research Institute of Fisheries Engineering [15]

Although in our previous experiment [14], the relationship between the drive frequency for this control and the wind velocity was adjusted by measuring the steady heel angle of the ship model under the non-fluctuating wind, the wind velocity was directly measured with a hot wire anemometer in this experiment. This wind measurement was executed without the ship model, and 15 measured points were used, as shown in Fig. 6. Further, the distance between the wind blower and the ship position was changed with the shift of the position of the blower.

These measured data, as shown in Fig. 7, the wind velocity gradually decreases with the distance from the blower. In this study, the data where the ship model position

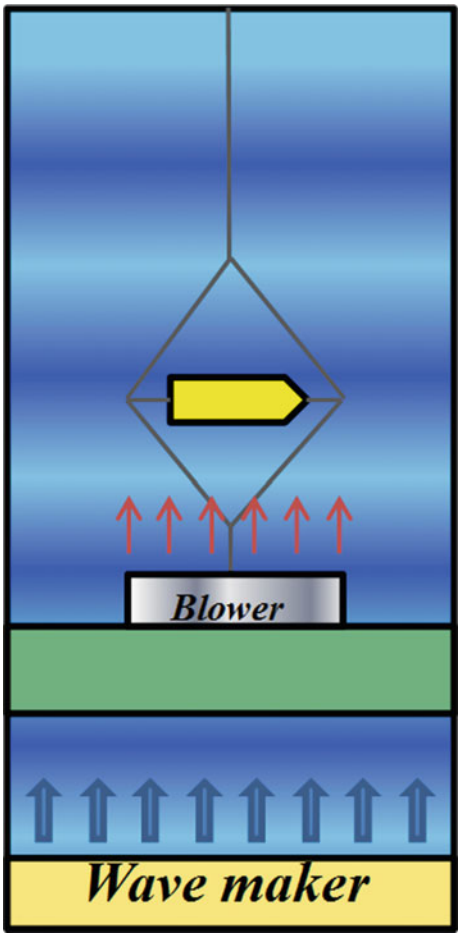

Fig. 2 Overviews of the experimental set-up

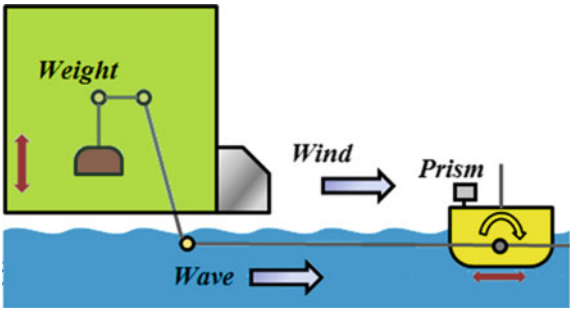

Fig. 3 Lateral views of the experimental set-up

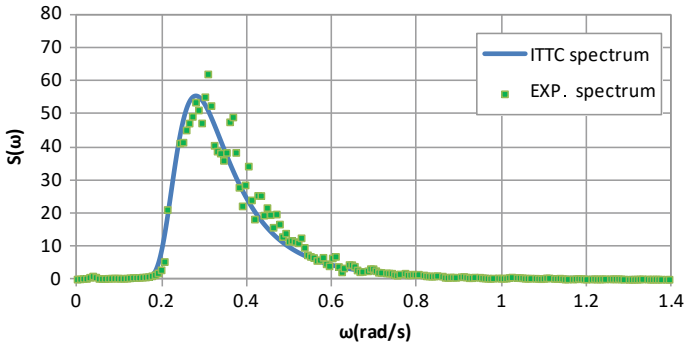

Fig. 4 Comparison of wave energy spectra

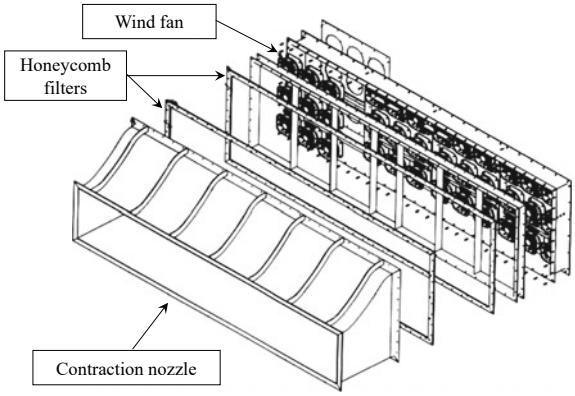

Fig. 5 Wind blower

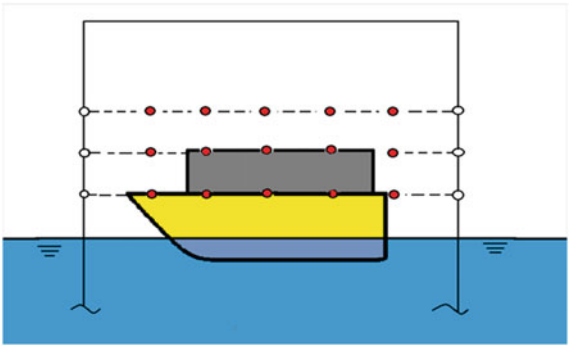

Fig. 6 Measurement points for wind velocity

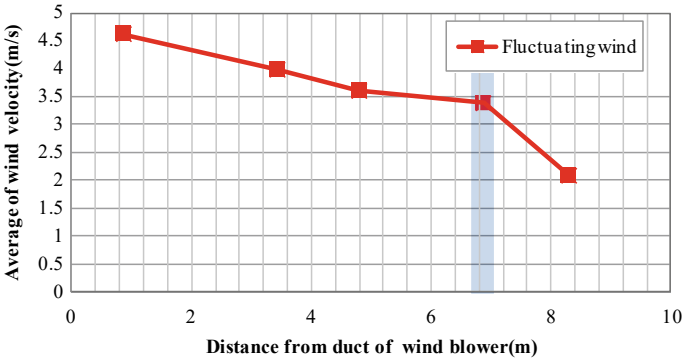

Fig. 7 Measured wind velocity as a function of distance from the blower. Here shaded zone indicates ship position during experiments in wind and waves

measured during the experiment is used so that the mean wind velocity used here is about 28 m/s in full scale.

The wind velocity has some spatial non-uniformness, as shown in Fig. 8, because the ratio of blower breadth to ship length of 1.327 is not so sufficiently large. The use of a wider blower or smaller ship model is preferable.

The wind velocity spectrum is designed with the Davenport spectrum [4] without the transfer function between the drive frequency and the wind velocity. Figure 9 shows one example of the comparison of wind velocity spectra. In this figure, the red line indicates the specified spectrum, and the blue diamond shape symbols indicate the measured one. From this figure, it can be seen that the measured spectrum was qualitatively similar to the specified one. In our previous experiment [14], a better agreement was obtained between the measured and specified spectra but with a mean

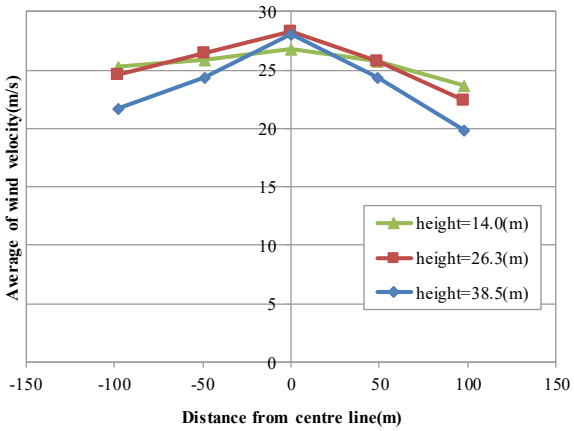

Fig. 8 Mean wind velocities measured at different positions

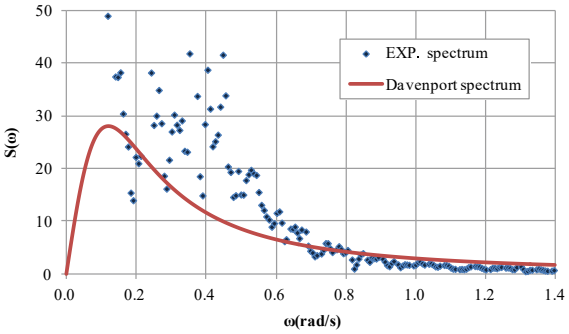

Fig. 9 Comparison of wind velocity spectra

wind velocity of 22.5 m/s. In the case of high wind velocity, it seems appropriate to take account of the transfer function. As to this problem, in our other study [20] conducted after this study, more detailed consideration was provided, and it was confirmed that the approach mentioned above is valid.

At present, in the National Research Institute of Fisheries Engineering, two units were added to the wind blower, the problem of the spatial non-uniformness shown in Fig. 8 was reduced [20].

3.2 Numerical Modelling

For a comparison with the model experiment, the uncoupled roll model [14] was used in this study. As recommended by the IMO [7], the nonlinear roll damping coefficients in calm water and the effective wave slope coefficient were estimated with roll decay model tests and the roll response model tests in regular beam waves, respectively. The wind-induced moment was estimated with the relationship with wind drag coefficient and heeling angle, which were directly measured with constant beam wind velocities on their own using the cable tension and the gyroscope. As shown in Figs. 10 and 11, the estimated wind drag and heel angle reasonably agree with the measured data so that the estimation of wind velocity from these ship data, which was used in our previous work [14], can be judged as reliable.

3.3 Comparison of Experiment and Simulation

Following the draft guidelines in 2013 [8], the ensemble average of the variance of roll angle obtained by the model experiment was compared with that by the numerical simulation with the confidential intervals using the significant level of 5%, i.e., 95% confidence interval, assuming the Gaussian distribution as shown in Fig. 12. Here 20 realisations were used for both model experiment and numerical simulation, and the

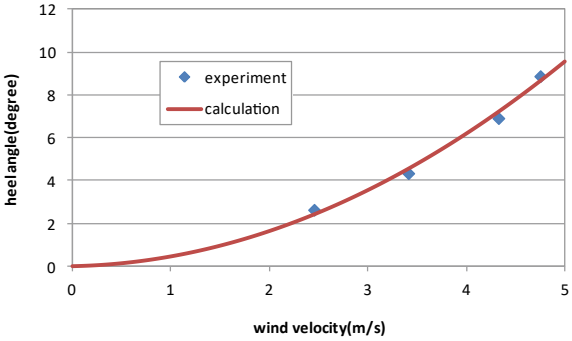

Fig. 10 Steady heel angle with constant wind velocity

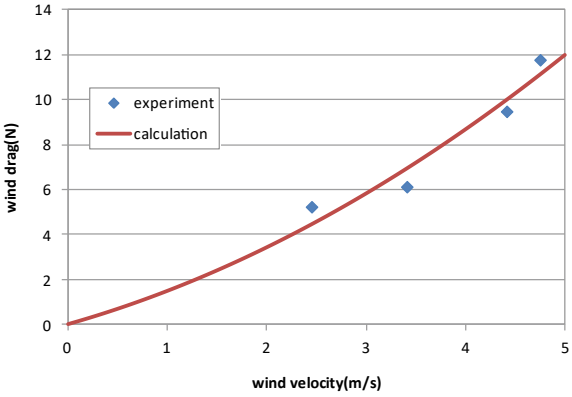

Fig. 11 Wind drag with constant wind velocity

duration is 3600 s in full scale. The initial heel angle due to cargo shift was 6 degrees towards the lee side because capsizing was not likely to occur without the initial heel angle. In the numerical simulation, the mean wind velocity was set to that from the mean of central points for wind velocity measurement except for the highest one. In the numerical simulation here, the measured wind velocity spectrum is used. Since the two confidential intervals are overlapped, we could conclude that the numerical model was validated with the model experiment. As reported in a separate paper [17], the measured roll spectrum in the same experimental campaign has a single peak at the natural roll frequency inside the region of external excitation due to wind and waves. The draft guidelines in 2013 requested a significant level of 1% for a synchronous roll, but the above suggests that the significant level of 5% seems to be reasonable.

As a next step, the comparison of capsizing probability between the model experiment and numerical simulations is shown in Fig. 13 with 95% confidence intervals using a binomial distribution [3]. Here three different ways of determining the mean wind velocity are used. The "simulation 2" indicates the way that used in the comparison of the variance of roll angles. The "simulations 1 and 2" use the mean of three points at the middle height and that of the central point at the middle height,

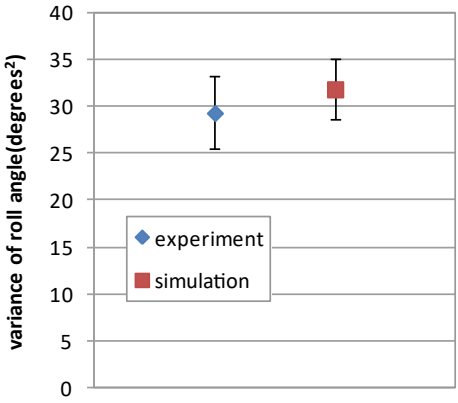

Fig. 12 Comparison of variance of roll angle between experiment and simulation

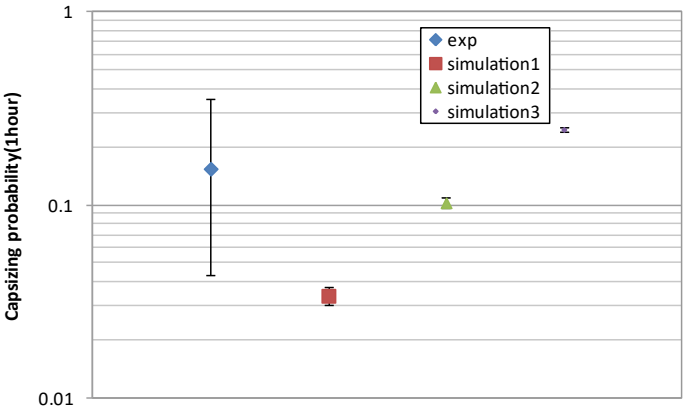

Fig. 13 Comparison of capsizing probability of experiment and simulation

respectively. The results indicate that both "simulation 2 and 3" shows acceptable agreement, and "simulation 1" provides a too low probability. Thus, the appropriate selection of measured points for wind velocity is crucial for validating numerical models with the width of the wind blower array taken into account.

4 Stability Failure Due to Pure Loss of Stability

For validating a numerical model for pure loss of stability in irregular astern waves, experiments using a 1/48.8 scaled model of the 154 m-long ONR flared topside vessel [1] were executed at the Marine Dynamics basin, as shown in Fig. 1, of National

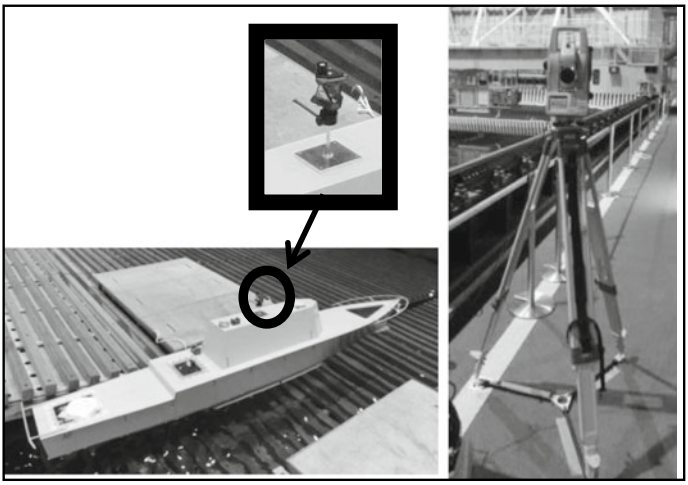

Fig. 14 Total station system (left; prism right; theodolite) used in the model experiment

Research Institute of Fisheries Engineering [15], based on the ITTC recommended procedure on intact stability model test [12]. The position of the ship model was observed by a total station system. It consists of the theodolite, which is an optical distance and direction measuring device, and the prism which reflects light rays from the theodolite is on the ship model, as shown in Fig. 14. The size of the prism is much smaller than the lateral projection area of the above water hull. By synchronising data of the total station system and gyroscope on the vessel, the ship position in the inertial coordinate system was obtained. Ship velocity was calculated by differentiating the position of the centre of gravity of the ship.

For precise comparison in time series between the experiment and the simulation, estimation of wave height at each ship position is indispensable. The wave elevation was measured by a servo-needle-type wave height meter near the wave maker. It was synchronised, by the trigger in radio signal, with the ship position data and the ship motions. The Fourier spectrum from these measured wave data was converted with the ship position data. Then it was inversely transformed so that the wave elevation at the ship position was obtained. This converted Fourier spectrum was also used for numerical simulation as its input.

The wave elevation at the ship's centre of gravity was calculated by the above procedure, and is shown in Fig. 15 in model scale with measured roll and pitch data. Here positive wave elevation indicates the movement downwards, the positive roll results in downward movement of the starboard side and positive pitch means bow up. This measured result indicates that the roll angle becomes large whenever the ship meets a wave crest, which is defined as the minima of the wave elevation. The measured roll period of 3.55 s, which is equal to the encounter wave period, is longer than the natural roll period of 2.95 s. These facts suggest that the typical behaviour known as pure loss of stability was relevant [10]. Here the significant wave height is

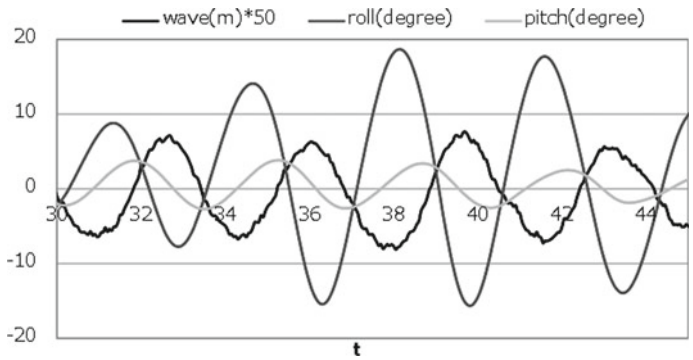

Fig. 15 Wave elevation at ship's centre of gravity and roll and pitch angle recorded in irregular waves shown in model scale

0.2066 m, the mean wave period is 1.627 s, the rudder gain is 1.0, the Froude number is 0.25, and the autopilot course from the wave direction is −15°. Earlier and similar procedures and results were published by Clauss and Hennig [2].

The numerical model proposed by Kubo et al. [13] is based on a nonlinear manoeuvring model with linear wave forces and nonlinear restoring variation. The manoeuvring, roll damping and propulsion coefficients were obtained by conventional model tests such as Circular Motion Test (CMT). The linear wave forces were estimated with a slender body theory with very low encounter frequency, and nonlinear restoring variation was predicted with Grim's effective concept and the Froude-Krylov assumption.

The numerical model mentioned above was applied to the experimental condition in Fig. 15. Figure 16 shows the comparison in time series between experiment and calculation in irregular waves. In this figure, the solid lines indicate the results of the model experiment, and the broken lines indicate the results of the calculation based on the numerical model, respectively. As shown in this figure, this numerical model well explains the present model experiment in irregular waves. This experimental procedure could be useful for developing guidelines for the validation of direct stability assessment once the acceptance standard is introduced for the failure modes of pure loss of stability at the IMO.

5 Concluding Remarks

The main remarks from this work are summarised as follows:

(1) For the failure mode of stability under dead ship condition, the experiment was executed by generating irregular waves and the fluctuating wind for a softly moored ship model. The number of capsizing was counted, and the capsizing

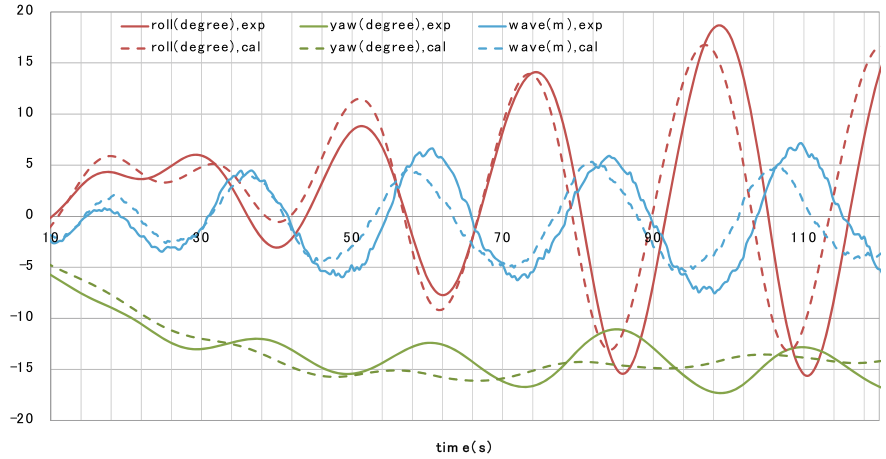

Fig. 16 Comparison in time series between experiment and calculation in irregular waves shown in full scale

probability was estimated with its 95% confidence interval. Here the adequate selection of representative wind velocity generated by wind fans is crucial.

(2) For the failure mode of pure loss of stability in stern quartering waves, the experiment was executed by generating irregular waves for the free-running ship model using autopilot. The ship angular motions and positions were measured by the gyroscope and the total station system, respectively. The incident wave elevation was measured by a wave probe fixed at a location of the model basin. Here the accurate Fourier transformation and reverse transformation of incident irregular waves are essential.

Acknowledgements This work was supported by a Grant-in-Aid for Scientific Research of the Japan Society for Promotion of Science (No. 24360355). It was partly carried out as a research activity of Goal-Based Stability Criterion Project of Japan Ship Technology Research Association in the fiscal year of 2013, funded by the Nippon Foundation.

This paper is an updated version of the paper read at the 14th International Ship Stability Workshop[19] with the latest information.

References

1. Bishop B, Belknap W, Turner C, Simon B, Kim J (2005) Parametric investigation on the influence of GM, roll damping, and above-water form on the roll response of model 5613, Report NSWCCD-50-TR-2005/027, Naval Surface Warfare Center/Carderock Division, West Bethesda, Maryland
2. Clauss GF, Hennig J (2004) Deterministic analysis of extreme roll motions and subsequent evaluation of capsizing risk. Int Shipbuild Prog 51(2/3):135–155

3. Clopper CJ, Pearson ES (1934) The use of confidence or fiducial limits illustrated in the case of the binomial. Biometrika 26(4):404–413
4. Davenport AG (1961) The spectrum of horizontal gustiness near the ground in high winds. Q J Metrol Soc 87:194–211
5. Hashimoto H, Umeda N, Matsuda A (2012) Broaching prediction of a wave-piercing tumblehome vessel with twin screws and twin rudders. J Mar Sci Technol 448–461
6. Hashimoto H, Umeda N (2019) Prediction of parametric rolling in irregular head waves. In: Belenky V, Spyrou K, van Walree F, Almeida Santos Neves M, Umeda N (eds) Contemporary ideas on ship stability. Fluid mechanics and its applications, vol 119. Springer, Cham, pp. 275–290
7. IMO (2006) Interim guidelines for alternative weather criterion, MSC.1/Circ. 1200, IMO (London)
8. IMO (2013) Information collected by the correspondence group on intact stability, submitted by Japan, SDC 1/INF.8, IMO (London)
9. IMO (2020) Interim guidelines on the second generation intact stability criteria, MSC.1/Circ. 1627, IMO (London), pp 1–60
10. IMO (2021) Report of the correspondence group (part 3), submitted by Japan, SDC 8/5.Add.2, IMO (London)
11. ITTC (1978) Report of Seakeeping Committee, Proceedings of the 15th ITTC
12. ITTC (2008) Recommended procedures, model tests on intact stability, 7.5-02-07-04
13. Kubo H, Umeda N, Yamane K, Matsuda A (2012) Pure loss of stability in astern seas—is it really pure? In: Proceedings of the 6th Asia-Pacific workshop on marine hydrodynamics, Johor, pp 307–312
14. Kubo T, Umeda N, Izawa S, Matsuda A (2019) Total stability failure probability of a ship in beam wind and waves: model experiment and numerical simulation. In: Belenky V, Spyrou K, van Walree F, Almeida Santos Neves M, Umeda N (eds) Contemporary ideas on ship stability. Fluid mechanics and its applications, vol 119. Springer, Cham, pp 591–603
15. NRIFE (2020) http://nrife.fra.affrc.go.jp/plant/kaiyou/kaiyou_e.html (Cited at 29 Sept 2020)
16. ShipStab (2021) http://shipstab.org/index.php/data-access/13-benchmarkingdata//11-cehipar2792-units (Cited at 22 Oct 2021)
17. Tsutsumi Y, Umeda N, Kawaida D, Matsuda A (2014) Probability of ship capsizing in beam wind and waves—comparison between model experiment and numerical simulation. In: Proceedings of the 7th Asia-Pacific workshop on marine hydrodynamics, pp 156–159
18. Umeda N, Izawa S, Sano H, Kubo H, Yamane K (2011) Validation attempts on draft new generation intact stability criteria. In: Proceedings of the 12th international ship stability workshop, pp 19–26
19. Umeda N, Kawaida D, Ito Y, Tsutsumi Y, Matsuda A, Terada D (2014) Remarks on experimental validation procedures for numerical intact stability assessment with latest examples. In: Proceedings of the 14th international ship stability workshop, pp 77–83
20. Umeda N, Matsuda A, Terada D (2015) Examination of guidelines for determining minimum propulsion power in the light of model experiment. In: Proceedings of international workshop on environmentally friendly ships, Yokohama National University